

# SmartPAN: A novel polysaccharide-microsphere-based surgical indicator of pancreatic leakage

Journal of Biomaterials Applications  
2020, Vol. 35(1) 123–134  
© The Author(s) 2020  
Article reuse guidelines:  
[sagepub.com/journals-permissions](http://sagepub.com/journals-permissions)  
DOI: 10.1177/0885328220913057  
[journals.sagepub.com/home/jba](http://journals.sagepub.com/home/jba)



Thomas Moritz Pausch<sup>1</sup> , Clara Mitzscherling<sup>1</sup>,  
Sepehr Abbasi<sup>1</sup>, Jiaqu Cui<sup>1</sup>, Xinchun Liu<sup>1</sup>, Ophelia Aubert<sup>1</sup>,  
Melanie Weissenberger<sup>1</sup>, Henrik Johansson<sup>2</sup>, Peter Schuisky<sup>2</sup>,  
Christopher Büsch<sup>3</sup>, Thomas Bruckner<sup>3</sup>, Mohammad Golriz<sup>1</sup>,  
Arianeb Mehrabi<sup>1</sup> and Thilo Hackert<sup>1</sup>

## Abstract

Postoperative pancreatic fistula is a major surgical complication that can follow pancreatic resection. Postoperative pancreatic fistula can develop as a consequence of leaking pancreatic fluid, which calls for an intraoperative indicator of leakage. But suitable indicators of pancreatic leakage have yet to be found. This study details the evidence-based development and early efficacy assessments of a novel pancreatic leakage indicator (SmartPAN), following the IDEAL framework of product development. We developed 41 SmartPAN prototypes by combining indicators of pancreatic fluid with a polysaccharide-microsphere matrix. The prototypes were assessed *in vitro* using porcine (*Sus scrofa domesticus*) pancreatic tissue and *ex vivo* with human pancreatic fluid. From these initial tests, we chose a hydrogel-based compound that uses the pH indicator bromothymol blue to detect alkali pancreatic fluid. This prototype was then assessed *in vivo* for usability, effectiveness and reliability using a porcine model. Treatment groups were defined by SmartPAN-reaction at initial pancreatic resection: indicator-positive or negative. Indicator-positive individuals randomly received either targeted closure of leakage sites or no further closure. We assessed SmartPAN's reliability and effectiveness by monitoring abdominal drainage for amylase and with relaparotomy after 48 h. SmartPAN responses were consistent between both surgical procedures and conformed to amylase measurements. In conclusion, we have developed the first surgery-ready indicator for predicting the occurrence of pancreatic leakage during pancreatic resection. SmartPAN can enable targeted prophylactic closure in a simple and reliable way, and thus may reduce the impact of postoperative pancreatic fistula by guiding peri- and post-operative management.

## Keywords

Pancreas, fistula, indicator, surgery, resection, IDEAL

## Introduction

Pancreatic resection (PR) is now widely regarded as a routine surgical procedure, with an estimated 40,000 annual operations in the United States.<sup>1</sup> PR is performed to treat a variety of malignant and benign conditions of the pancreas and can be combined with adjuvant chemotherapy to improve survival in patients with pancreatic adenocarcinoma.<sup>2,3</sup> Yet despite broad and consistent improvements, PR is still associated with appreciable morbidity and mortality.<sup>4</sup> An important complication is the development of postoperative pancreatic fistula (POPF), which involves leakage of

enzyme-rich pancreatic fluid from the surgical remnant or anastomosis. This leakage can lead to the breakdown of intra-abdominal tissue and result in sepsis,

<sup>1</sup>Heidelberg University Hospital, Heidelberg, Baden-Württemberg, Germany

<sup>2</sup>Magle Chemoswed, Malmö, Sweden

<sup>3</sup>Heidelberg University, Heidelberg, Baden-Württemberg, Germany

### Corresponding author:

Thomas Moritz Pausch, Heidelberg University Hospital, Im Neuenheimer Feld 110, Heidelberg 69120, Baden-Württemberg, Germany.  
Email: thomas.pausch@med.uni-heidelberg.de

hemorrhage or death.<sup>5,6</sup> POPF has been reported to affect up to 45% of patients following PR, and is associated with expensive hospital stays and significant economic burdens.<sup>7–13</sup>

High concentrations of pancreatic enzymes in fluid from the peripancreatic environment are highly predictive of POPF development after pancreaticoduodenectomy and distal pancreatectomy.<sup>14,15</sup> The pancreatic parenchyma is delicate and therefore requires a fastidious surgical technique to close the remnant or perform anastomosis. Leakage of pancreatic fluid during early recovery is considered to be caused by intraoperative factors such as disruption of pancreatic ducts or incomplete closure of the pancreatic remnant.<sup>5,6,16</sup> However, it is difficult to identify potential pancreatic leaks during surgery as the fluid is clear and seeps from microscopic openings into a moist environment. Thus, identifying and localizing pancreatic leakage would likely optimize peri- and post-operative management, including placement of drains, targeted closure, and proper postoperative care. Consequently, the extent of pancreatic fluid leakage and the risk of POPF may be reduced.

At present, there are no reliable ways to predict POPF, take prophylactic peri-operative measurements or perform targeted closure during surgery.<sup>16</sup> Some attempts have been made to develop a method for intraoperative identification of pancreatic fluid leakage,<sup>17–21</sup> but none are clinically useful. The ideal indicator of pancreatic fluid leakage would show high sensitivity and specificity *in situ* with a clear and discernible reaction. Further, it would be quick and easy to use in an operating environment, requiring basic training. Other essential characteristics include a durable and localized response, absence of toxicity, and low cost. In this study, we describe the development of a reliable intraoperative pancreatic fluid leakage indicator (SmartPAN) that may facilitate targeted closure of the pancreatic remnant and allow prediction of POPF development.

## Methods

The study was performed in two parts, using the IDEAL Framework for product development (Idea, Development, Exploration, Assessment, Long-term monitoring).<sup>22–24</sup> Part 1 covers the refinement of an effective pancreatic fluid indicator (SmartPAN). Our biomaterial is based on a microsphere-hydrogel-carrier-matrix that accurately locates leaks by exploiting the alkali pH of pancreatic fluid. We developed a proof-of-concept for SmartPAN with *in vitro* and *ex vivo* experimentation. Part 2 covers a 48-hour *in vivo* evaluation of usability, effectiveness, and safety using a porcine model (*Sus scrofa domesticus*).

### Part 1: Identification, refinement, and preliminary testing of SmartPAN

**Assessing candidate indicators.** We tested four different substances for use as the active indicator (Table 1). The Phadebas<sup>®</sup> amylase test (Phadebas, Kristianstad Sweden) and tri-iodide-starch solution (Pharmacy Department, Heidelberg University Hospital) were selected because they identify amylase, a natural component of pancreatic fluid. Bromothymol blue (BTB) and phenolphthalein were selected because they are indicators of alkali solutions, as pancreatic fluid has a pH of 8.0–8.3 whilst human blood has approximately 7.4.<sup>25</sup>

We applied these indicators in their raw form to (i) saliva-moistened filter paper ( $n=3$  per indicator; 1 mL indicator applied),<sup>26</sup> (ii) fresh porcine pancreatic tissue obtained from slaughterhouse pigs ( $n=5$  per indicator; 2–3 mL SmartPAN per slice in a homogenous layer), (iii) human pancreatic fluid obtained from surgery ( $n=3$  per indicator; 2 mL SmartPAN applied to 100  $\mu$ L pancreatic fluid on  $3 \times 3 \text{ cm}^2$  gauze), and (iv) *in vivo* using pigs ( $n=10$ , indicators applied haphazardly). Indicator responses were qualitatively evaluated *in situ* for (i) contrast of color change against the background, (ii) visual resolution (amount of pancreatic fluid needed for visualization), (iii) time-to-reaction (shorter is better), and (iv) practical handling. Based on these trials, we selected BTB as the active indicator.

**The polysaccharide-microsphere-carrier-matrix.** SmartPAN was created by combining the active indicator (BTB) with a cross-linked potato-starch derived polysaccharide-microsphere-matrix (Magle Chemoswed, Malmö, Sweden), specially designed to absorb and electrostatically bind to the indicator (Figure 1; Table 2). The microspheres were prepared with a water-in-oil emulsion technique, using epichlorohydrin as a cross-linking agent. The polysaccharide microspheres have a dual function as a carrier for the indicator and as a structural vehicle to concentrate reactions at leakage sites. That is, the microspheres rapidly concentrate aqueous pancreatic fluid, due to the hydrophilic nature of starch, and expose the dissolved constituents to the indicator. Upon contact with alkali pancreatic fluid, the indicator reacts with a rapid and intense color change that visualizes pancreatic fluids close to the site of origin. Because the indicator has low solubility it does not osmotically shift from the matrix, thereby allowing localized reactions. Following use, the microspheres degrade through enzymatic action to biocompatible glucose within minutes.

We provide a chemical characterization of the microspheres in the Supplementary Information. In brief, we used magic angle spinning nuclear magnetic

**Table 1.** Substances tested as indicators of pancreatic fluid.

Indicator	Responds to	Color change	Mode of action
Phadebas Amylase Test <sup>©</sup>	Amylase	Clear to blue	Cleavage of dye from the starch matrix by amylase
Triiodide-starch solution	Amylase	Blue to clear	Cleavage of starch in tri-iodide-starch-complex by amylase
Bromothymol blue (BTB)	pH >7.6	Yellow to green/blue	Deprotonation
Phenolphthalein	pH >8.2	Clear to pink	Deprotonation

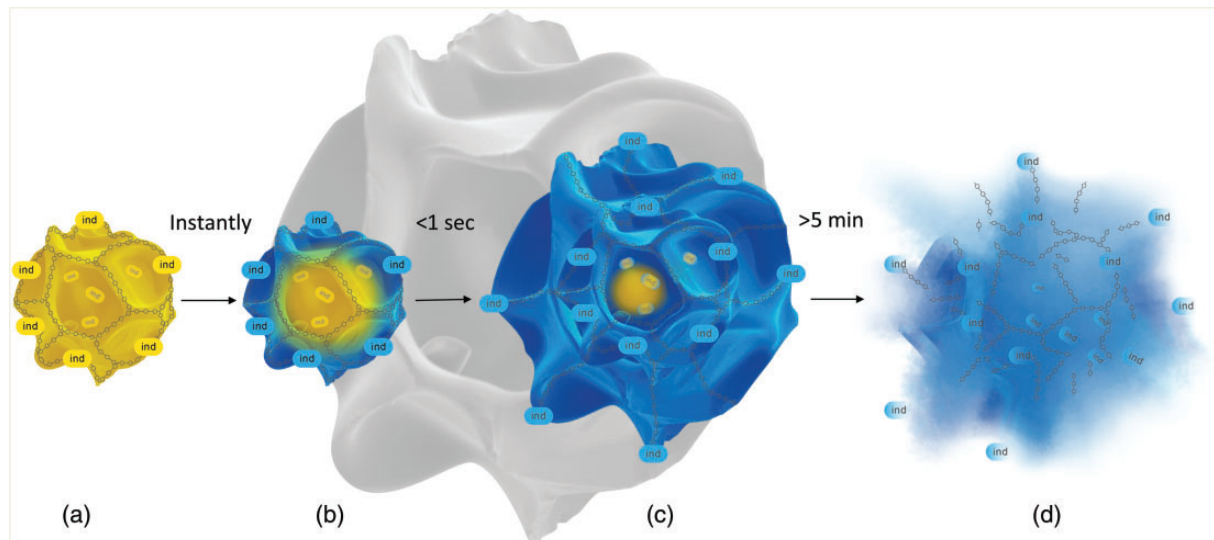


**Figure 1.** Microsphere-matrix mode of action. (a) Sponge-like polysaccharide microspheres with bromothymol blue (BTB) bound to its surface and within its matrix. (b) Immediate surface color change in reaction to alkali pancreatic fluid. (c) Pancreatic fluid reaches the microsphere core and the indicator within, causing local fixation and intensification of the reaction within microseconds. (d) Pancreatic amylase hydrolyses the polysaccharide matrix of biocompatible SmartPAN within minutes. Photo credits TP. The faded background microsphere shows an original electron microscope photo of the microsphere courtesy of Magle Chemoswed, Malmö, Sweden.

resonance, X-ray powder diffraction, and scanning electron microscopy. These techniques demonstrate that the microspheres are a hydrolyzed, glucose-based, carbohydrate polymer based on starch. The microspheres are less rigid than native starch, and biodegrade faster owing to their amorphous structure. The chemical compound forms a smooth sphere with a diameter of 200–250 µm.

**Refining the indicator prototype.** We tested the BTB-microsphere compound with wipe, tape, powder, and hydrogel applicators, resulting in 20 different SmartPAN prototypes (SmartPAN 001–020, details available upon request). The prototypes were assessed (i) *in vitro* on slices of freshly resected porcine pancreas during surgery ( $n=5$  per indicator; 2–3 mL SmartPAN per slice in a homogenous layer), (ii) *ex vivo* with fresh human pancreatic fluid ( $n=3$ –12 per indicator; 2 mL SmartPAN applied to 100 µL pancreatic fluid on  $3 \times 3 \text{ cm}^2$  gauze), and (iii) *in vivo* with pigs ( $n=10$ ; 4 mL SmartPAN applied to freshly resected pancreatic

stump). Representative images of testing are given in Figure 2.

The prototypes were assigned a subjective performance rating of 0 (undesirable) or 1 (desirable) by the attending surgeon for: (i) handling (desirable compounds are easy to use, homogenous and viscous enough to remain in place), (ii) reaction time (desirable compounds react within seconds), (iii) power (desirable compounds have an intense reaction without background interference), (iv) precision (desirable compounds react only over leakage sites), (v) durability (desirable compounds maintain their structure and have a stable, persistent, and localized color change for many minutes). We summed these scores for a total performance rating out of 5 and selected the best as a “gold standard” to use throughout the remainder of the trials. We developed a further 21 subtypes from the gold standard (SmartPAN 021–041) and tested them *in vitro* with porcine pancreatic tissue to ensure homology among types ( $n=5$  per indicator).

**Table 2.** Particle characteristics and *in vivo* surgical performance scores for the four gold standard SmartPAN subtypes. All subtypes have gel-like surface properties when swollen in aqueous solution. They may also have a slightly negative surface charge from hydroxyl groups. Particles degrade in 4–24 h.

Property	SmartPAN 016	SmartPAN 026	SmartPAN 032	SmartPAN 039
Applicator	Gel	Gel	Gel	Gel
Starch-matrix concentration (%w/w)	16.7	14.9	15.3	14.7
Particle size range ( $\mu\text{m}$ )	50–1200	50–1200	50–1200	32–900
Particle shape	Spherical	Spherical	Spherical	Spherical
Degree of crosslinking (mol %)	26	26	26	27
Buffered	Y	Y	Y	Y
Buffer concentration (mMol)	18	6.6	1.5	1.4
Indicator concentration (%w/w)	0.050	0.045	0.045	0.044
Ion strength (mMol)	190	167	157	157
pH	4.7	4.8	4.5	4.4
Sterilized	N	Y	Y	Y
Performance: handling	I	0	I	0
Performance: reaction time	I	I	I	I
Performance: power	I	0	I	I
Performance: precision	I	I	I	I
Performance: durability	I	I	I	I
Performance: total	5	3	5	4

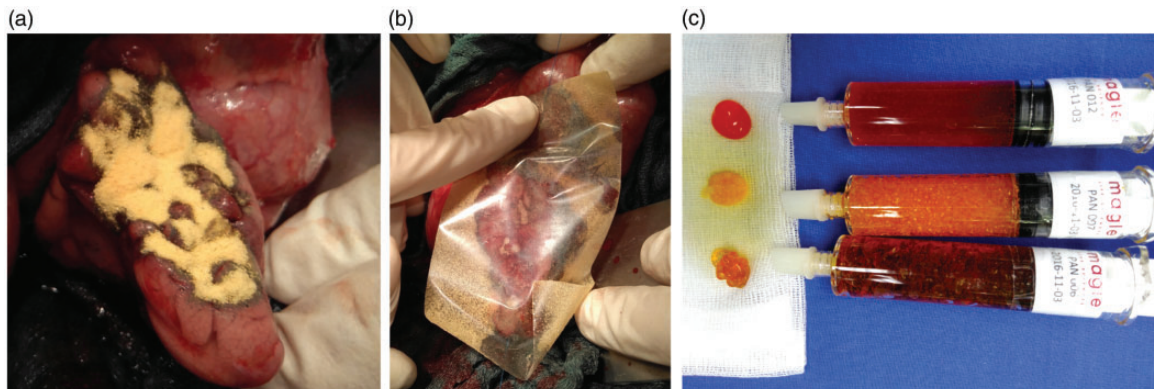


**Figure 2.** Testing SmartPAN prototypes: (a) powder *in vivo*; (b) tape *in vivo*; (c) hydrogel *in vitro*. Photo credits TP.

**SmartPAN gold standards.** The final SmartPAN hydrogel prototype was created by mixing 121 g (746 mMol, based on the monomeric unit) of dry microspheres with 121 mL of 0.3% BTB/ethanol solution and drying overnight at 60°C in a vacuum oven. A total of 15 g of the dry mixture was then swelled in 83 mL of saline, containing 1.5 mL of 1 Mol phosphate buffer (pH = 5.8) per liter saline. The pH was adjusted to 4.5–4.7 with 0.1 Mol HCl acid. We measured the pH of the gel during and after the addition of saline/buffer with a pH electrode in a sediment mixture of 1.0 g of gel and 5.0 mL of purified water. We measured the buffer capacity of the gel after the addition of saline/buffer by treating the mixture with 3.60 mL of 0.001 Mol NaOH that had been allowed to sediment. Sterilized compounds were created by steam autoclaving

hydrogel-filled syringes. This did not change the pH or consistency of the gel but did slightly increase the buffer capacity.

As part of the product development, we qualitatively and subjectively compared SmartPAN to potentially equivalent products in the literature following the guidelines from the European Commission for the development of medical devices.<sup>27</sup> We find that there are similar products, but none that are fully equivalent to SmartPAN (Table 3; full results available upon request).

## Part 2: In vivo assessment of SmartPAN usability and effectiveness

**Animal treatment groups.** Ten pigs underwent distal pancreatectomy as described below, and the pancreatic

remnant was assessed for pancreatic leakage after closure. The animals were grouped according to indicator reaction: “indicator-positive” ( $n=9$ ) and “indicator-negative” ( $n=1$ ). Animals in the “indicator-positive” group were randomly sub-grouped by coin toss into two groups based on whether the leakage was left uncorrected (leakage-uncorrected;  $n=7$ ), or treated with targeted closure using extra sutures (leakage-corrected;  $n=2$ ). This resulted in three study groups, summarized in Table 4. In order to minimize inter-observer variance, indicator responses were agreed upon by the entire operation team present during each procedure.

**Confirming SmartPAN usability in vivo over 48 h.** The usability of the four gold standard SmartPAN formulations (SmartPAN 016, 026, 032, 039) was assessed *in vivo* with distal pancreatectomy. Following the operation, we conducted a clinical and laboratory follow-up assessment of pancreatic leakage by measuring

**Table 3.** Equivalent products for detecting pancreatic leakage. Clinical, technical, and biological equivalence scored as 1: doubtful equivalence, 2: probable equivalence, 3: high equivalence, following MEDDEV guidelines.<sup>27</sup> Level of evidence (LoE) scored according to guidelines from the American Heart Foundation, with 1 being the highest and 8 being the lowest.<sup>28</sup> A score of 3 indicates a prospective, nonrandomized controlled study, and a score of 6 indicates animal experimental studies, mechanistic models, or *in vitro* studies. N refers to the number of subjects studied.

Product	Equivalence				
	Clinical	Technical	Biological	LoE	N
Bromothymol blue <sup>29</sup>	2	2	2	3	46
Litmus paper <sup>20</sup>	3	2	1		
Fluorescent probe <sup>18,19,21</sup>	3	2	1	6	30
FRET-based nanoprobe <sup>17</sup>	3	2	1	6	6

FRET: Förster resonance energy transfer.

enzyme levels in blood serum and abdominal drainage fluid. Abdominal fluid and blood samples were obtained from the study animals at the initial operation on day 0 and again on the mornings of days 1 and 2. Immediate analysis was performed at the central laboratory of Heidelberg University Hospital.

According to the guidelines of the International Study Group of Pancreatic Fistula (ISGPF), pancreatic leakage in humans can be predicted by blood serum amylase values  $\geq 3$  times the upper normal serum level at day 3 after surgery.<sup>6</sup> Because serum amylase levels vary significantly between different breeds and ages of pig, we calculated a mean value of all day 0 readings to serve as a “normal” amylase level. We then calculated the ratio of abdominal drainage fluid: normal serum amylase content for each pig, and considered values  $\geq 3$  as indicative of potential leakage. As this study was only 48 h, these data are presented only as supporting evidence for leakage rather than a true diagnosis for leakage or POPF.

After 48 h of follow-up, the pigs were relaparotomized by removing sutures and assessed for intra-abdominal complications such as ascites, adhesions, signs of infection, and bleeding. The stump of the pancreatic remnant was closely assessed for signs of infection, bleeding, pancreatitis, and inadequate closure. We then reapplied SmartPAN to the surface of the pancreatic remnant. The animals were euthanized at the end of the experiment by central venous application of potassium-chloride whilst conducting deep narcosis and analgesia.

#### Surgical procedure: Distal pancreatectomy and closure

The same surgeon operated in all cases to ensure standardization of technique. Distal pancreatectomy was performed under general anaesthesia in semi-sterile conditions. A central venous catheter was placed into the jugular vein for postoperative blood sampling and administering medication. An upper median

**Table 4.** Surgical assessment and treatment group assignment following application of SmartPAN at initial surgery.

Treatment group	SmartPAN subtype	Indicator reaction
Group 1 ( $n=7$ ): leakage-uncorrected	16	Leakage at one site mid-stump
	26	Small leak adjacent to the cranial suture
	32	Light but diffuse leakage
	39	Leakage at two sites cranial-stump
	39	Leakage at two sites cranial-stump
	39	Leakage at cranial and mid-stump
	39	Diffuse light leakage
Group 2 ( $n=2$ ): leakage-corrected	16	Leakage at caudal-stump
	26	Two leakages adjacent to original sutures
Group 3 ( $n=1$ ): indicator-negative	32	No leakage

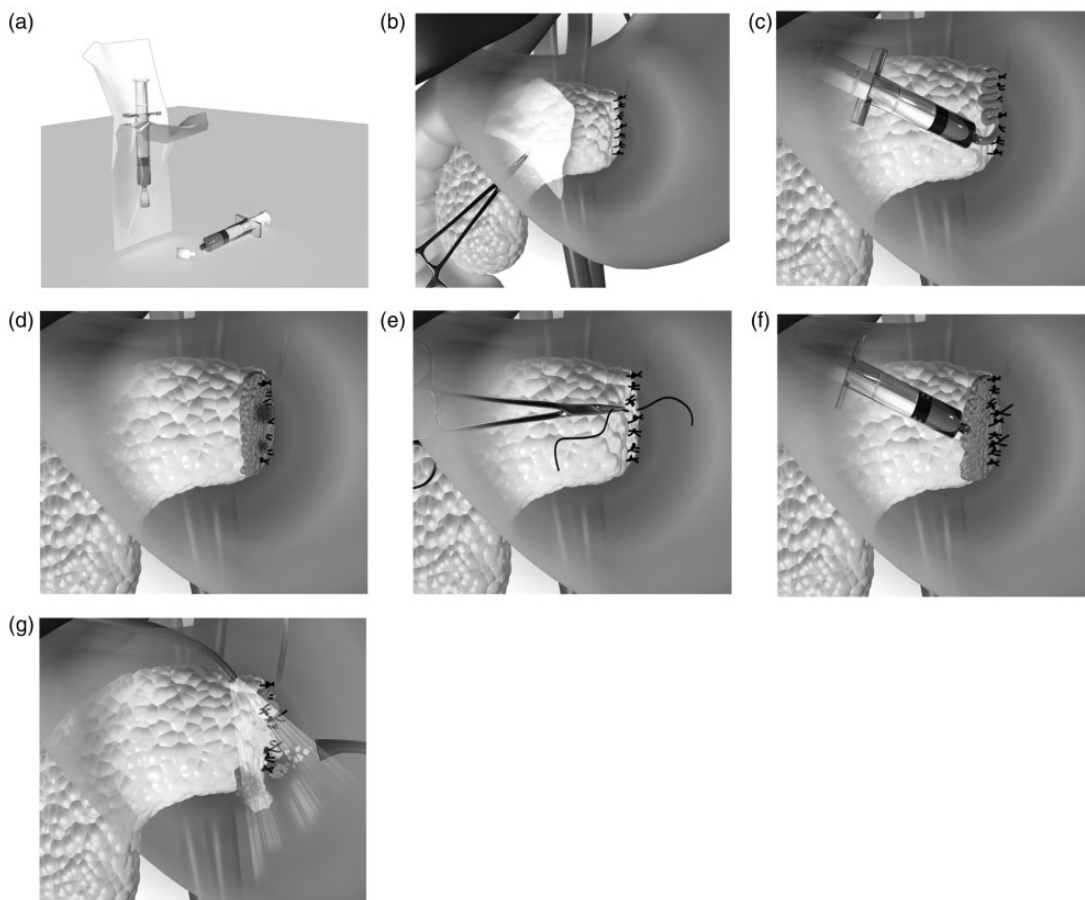


**Figure 3.** Directions for SmartPAN application. (a) Remove applicator from packaging. (b) Prepare the application site by exposing the organ, performing hemostasis, and cleaning away blood and liquid by rinsing and dabbing. (c) Apply SmartPAN in one continuous layer to the tissue surface, keeping the applicator jet pointed downward. Move the applicator back and forth over the tissue in an S-shaped pattern. (d) Check for indicator reaction. If negative, remove SmartPAN by rinsing with sterile isotone saline, and reapply for verification. (e) If indicator is positive, perform targeted surgical closure. (f) Reapply SmartPAN to confirm closure. (g) Rinse the surgical site and remove SmartPAN fluid with drainage or suctioning. Images courtesy of Magle Chemoswed, Malmö, Sweden.

laparotomy incision and opening of the omental bursa exposed the pancreas. Scissors were used to release the splenic lobe (2–3 cm from the pancreas edge) from the surrounding peritoneal tissue and renal fascia. Pancreatic tissue was then resected using a scalpel, sliced and immediately used for *ex vivo* experimentation. Pancreatic hemostasis was achieved using a maximum of three single/x-stitch, nonabsorbable sutures. The pancreatic stump was closed using transverse, nonabsorbable single sutures (1 suture/cm tissue), and then rinsed with sterile saline and dried with sterile gauze.

Indicator prototypes were applied to the pancreatic stump (Figure 3). Prior to application, the operative field was gently rinsed and dabbed to free the area from fluids that might reduce effectiveness. The presence of water moisture did not appear to impair SmartPAN function. The tissue of interest was maintained in a horizontal position and approximately 4 mL

of SmartPAN was applied rapidly and uniformly to the cut surface from above, taking care to prevent over-spill. It was not necessary to rinse the SmartPAN unless its presence hindered surgical procedure.

Pigs used for the *in vivo* component of Part 1 received no further treatment after SmartPAN application and were euthanized after testing. For Part 2, a closed suction drain (Jackson Pratt<sup>®</sup>) was placed next to the pancreatic stump and passed through the sub-costal abdominal wall to evacuate peritoneal fluid and use it for further analysis. Pigs that expressed a positive-indicator response and were assigned to the leakage-corrected group received a fine-closure of the stump using one targeted nonabsorbable single/x-stitch suture. The effectiveness of closure was then tested with reapplication of SmartPAN. Pigs in the leakage-uncorrected group received no targeted closure. We finished the operation by closing the abdominal wall

with continuous suturing of the fascia and skin. At 48 h after surgery, pigs were relaparotomized for clinical evaluation and re-application of SmartPAN, then euthanized.

### Materials and subjects

**Procurement of porcine pancreatic tissue and human pancreatic fluid.** Porcine pancreatic tissue was donated by a local slaughterhouse (Fleischversorgungszentrum, Mannheim) within 12 h post-mortem, and stored at 2°C until required (see Part 1: Assessing candidate indicators). We also used resected tissue from *in vivo* experiments for immediate *in vitro* testing (see Part 1: Refining the indicator prototype).

The human pancreatic fluid was retrieved from fresh surgical specimens for immediate use, after first obtaining informed consent from the patient in accordance with the Declaration of Helsinki (approved by Heidelberg University Ethics Committee; votes 301/2001, 159/2002). A series of four patients received partial pancreatectomy due to malignant pancreatic tumors and we aspirated fluid from surgical specimens for testing next to the operation table.

**Porcine subjects.** Twenty female German domestic pigs (*Sus scrofa domesticus*) were used in this experiment due to their close anatomic and metabolic homology to humans. The animals were approximately 30 kg in weight and three months of age. Their physical and clinical well-being was monitored closely throughout the trial by trained animal keepers and veterinarians. The animal experiments performed in this study were governmentally approved according to German regulations of the Animal Welfare Act (TierSchG § 8 Abs.1), and Regierungspräsidium Karlsruhe (File 35-9185.81/G-184/16). We adhered to all applicable

codes of practice for the housing, care and humane killing of animals used in scientific procedures.

**Statistical analysis.** We used SPSS (IBM Corp. Released 2017. IBM SPSS Statistics for Windows, Version 25.0. Armonk, NY: IBM Corp.) for statistical analysis of abdominal drainage fluid data. Differences in amylase concentration between groups were assessed with a Kruskal-Wallis test for omnibus comparison, followed by exact Mann-Whitney U tests with a Bonferroni correction for pairwise comparisons. We considered  $p < 0.05$  (0.017 with correction) as statistically significant. We recorded missing values in cases where animals did not yield sufficient drainage fluid or central venous blood for laboratory analysis. We also calculated sensitivity and specificity for the predictive qualities of SmartPAN.

### Results

#### Part 1: Identification, refinement, and preliminary testing of SmartPAN

**Assessment of candidate indicators.** We summarize the test results and conclusions of candidate indicators for SmartPAN in Table 5. Based on these findings, the pH indicator BTB was selected as the most appropriate indicator to combine with the polysaccharide-microsphere-matrix.

**Refining the indicator prototype.** We developed SmartPAN by combining BTB with the polysaccharide-microsphere-matrix. The resultant product is a gel-like substance that expresses local color change from yellow to green/blue upon exposure to pancreatic fluid (Figure 4). Powders were difficult to handle, were too thick and were washed away by pancreatic fluid. Similarly, powdered tape also washed away.

**Table 5.** Performance of pancreatic fluid indicator candidates.

Indicator	Result	Conclusion
Phadebas Amylase Test <sup>©</sup>	Clear blue coloration specific to pancreatic fluid <i>in vitro</i> and <i>in vivo</i> . But only indirect coloration on the back of carrier sheets due to technical reasons.	No precise localization of pancreatic leakage possible.
Triiodide-starch solution	Specific color change for pancreatic fluid <i>in vitro</i> and <i>in vivo</i> . Direct reaction on pancreatic tissue. But an unfavorable color change from black to colorless fluid is hard to discriminate.	Does not enable clear visualization of pancreatic leakage.
Phenolphthalein	Specific color change for pancreatic fluid <i>in vitro</i> and <i>in vivo</i> . But unfavorable color change to pink above flesh is hard to discriminate.	Does not enable clear visualization of pancreatic leakage <i>in vivo</i> .
Bromothymol blue	Clear color change from yellow to green/blue for pancreatic fluid <i>in vitro</i> and <i>in vivo</i> . The effect is rapid and contrasts with surrounding body fluids.	Provides a clear and localized indication of pancreatic leak during surgery.

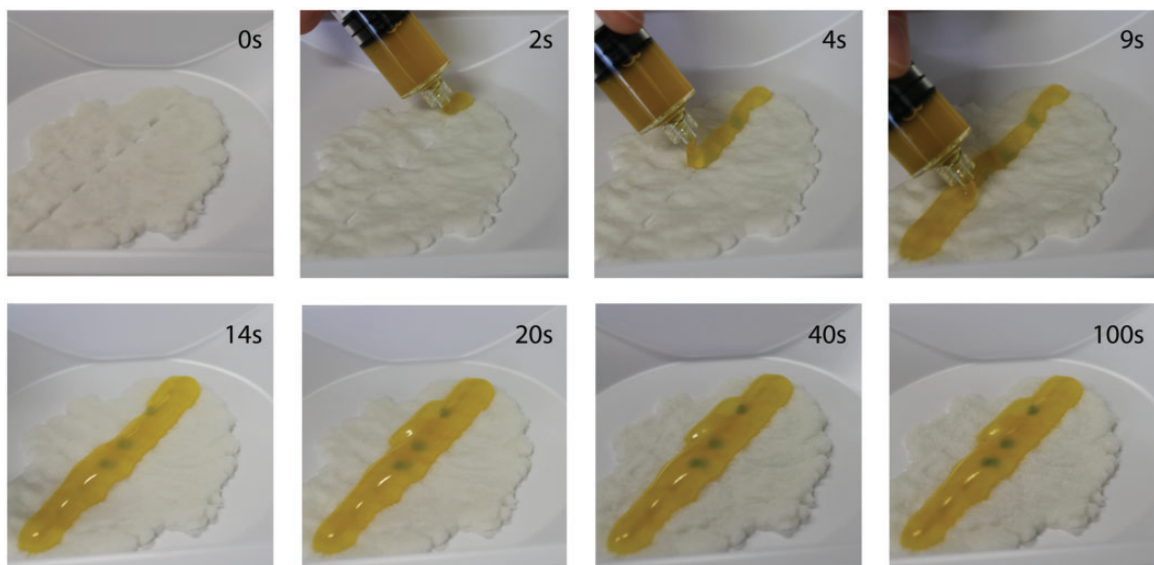


**Figure 4.** Identification of artificial leakage from local deposits of pancreatic fluid using SmartPAN hydrogel. Images courtesy of Magle Chemoswed, Malmö, Sweden.

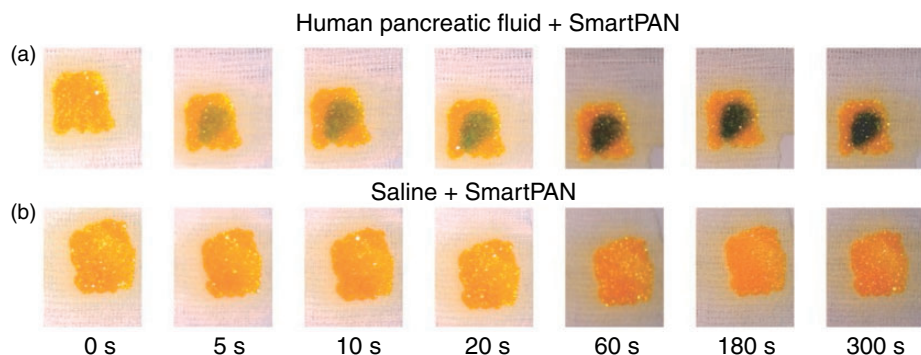


**Figure 5.** Ex vivo reactions of SmartPAN 016 on gauze over 300 s following application of: (a) 100 µL fresh human pancreatic fluid or (b) 100 µL saline (NaCl 0.9%). Photo credits TP.

Wipers were also ineffective, as they required a lot of pancreatic fluid to display a reaction. Prototypes that used a hydrogel applicator showed the best results, after refining the biomaterial properties (results available upon request).

The hydrogel-based SmartPAN 016 showed the greatest effectiveness of the 20 initial prototypes, providing a distinct localized color change with high visual resolution (small amounts of pancreatic liquid are needed for a clear color change). The reaction occurred in a short space of time and was sustained for a period  $>5$  min (Figure 5). SmartPAN 016 achieved a total performance score of 5/5 (Table 2). The full results of these tests are available upon request.

We conducted swelling experiments to determine how much liquid the microspheres can absorb.

The SmartPAN microsphere compound had a swelling capacity of 9 mL/g in purified water and 7.5 mL/g in isotone-saline. 90% of the swelling occurred within the first 60 s, and no more swelling occurred after 1 h.

Regarding the formulation of SmartPAN, there was a trend in buffer capacity and performance. Gels that had a buffer pH of 7.0–7.2 reacted quickly, whilst gels with pH  $>7.2$  overreacted and those with pH  $<7.0$  were slow. For optimal indication, the pH of the gel should be 4.4–4.6 and have a buffer capacity of pH 7.0–7.2. Unbuffered compositions were less precise with leakage detection. Further, compositions with high buffer strength provided somewhat slow detection, whereas buffer strengths of 1–10 mMol provided quick and precise leakage detection. We found that a degree of cross-linking around 26% Mol provided the composition

with proper resistance to amylase degradation (i.e. stability for >5 min). Furthermore, the amount of microspheres in the composition affects the viscosity of the composition. It was concluded that <10% w/w microspheres resulted in compositions that were too liquid, whereas >20% w/w were too thick. However, a concentration of 13–18% w/w provided a composition that was easy to handle and reacted quickly. We preferred to keep the BTB concentration as low as possible, but sufficiently high enough to provide clearly visible leakage detection. A concentration of BTB <0.04% w/w provided somewhat weak, but visible coloration.

At the conclusion of these trials, we designated SmartPAN 016 as the “gold standard”. We further developed 21 subtypes of SmartPAN 016 (SmartPAN 021–041), which were reassessed *in vitro* to ensure homology with SmartPAN 016 (results available upon request). We highlight four subtypes that showed desirable performance and homology with SmartPAN 016 *in vitro*. We hence classed them as equivalent to the gold standard and carried all four formulations to Part 2 (Table 2).

We also conducted preliminary *in vitro* cytotoxicity tests using HPDE and FAMPAC cells (results available upon request, article in preparation). These tests indicated that BTB had no toxicological effects on pancreatic cells up to three times the concentration found in SmartPAN.

## Part 2: *In vivo* assessment of SmartPAN usability and effectiveness

**Confirmed usability of SmartPAN gold standard *in vivo*.** The *in vivo* surgical usability scores for the four subtypes are shown in Table 2. All four subtypes scored overall usability scores  $\geq 3$ , reaffirming the performance of SmartPAN 016 as an indicator for pancreatic fluid and demonstrating sufficient homology between subtypes. Importantly, SmartPAN gold standards were deemed biocompatible and nontoxic in the context of this experiment. Specifically, the only nonphysiologically degradable compound is BTB, which was not detectable in abdominal drainage after 48 h (results available upon request, article in preparation). We believe that BTB is rapidly evacuated via surgical drainage. The microspheres, by contrast, are designed to biodegrade into glucose.

**Treatment groups differ in abdominal amylase levels.** The amylase content of the abdominal drainage fluid was measured on days 0, 1, and 2 to monitor for signs of pancreatic leakage (Table S1). Kruskal–Wallis tests indicated that there were no significant differences in amylase content between groups on any day

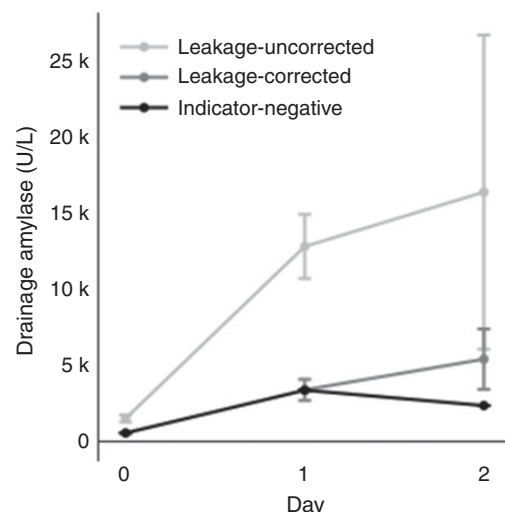


**Figure 6.** Mean  $\pm$  SE amylase levels (U/L) in abdominal drainage for treatment groups pre-pancreatectomy (day 0) and for two days post-pancreatectomy (black: indicator-negative; med grey: leakage-corrected; light grey: leakage-uncorrected).

(day 0:  $H_1 = 2.00$ ,  $n = 5$ ,  $p = 0.157$ , only missing values for group 2; day 1:  $H_2 = 5.73$ ,  $n = 10$ ,  $p = 0.057$ ; day 2:  $H_2 = 2.49$ ,  $n = 9$ ,  $p = 0.288$ ). However, the mean amylase content of drainage fluid was greatest in treatment-uncorrected pigs on days 1 and 2 post-operation, although not significantly after Bonferroni correction (Figure 6; Table 6). There were no significant differences in amylase content between treatment-corrected and indicator-negative pigs on days 1 or 2 (Figure 6; Table 6).

The baseline serum amylase level for this study was established to be 2178.6 U/L (min = 1335 U/L, max = 3303 U/L). This value was used to calculate ratios of abdominal drainage amylase: normal serum amylase, which can indicate the presence of pancreatic leakage (Table S1). Leakage-uncorrected pigs had ratios  $\geq 3$  for 7/7 pigs on day 1 and 3/6 pigs on day 2. By contrast, no leakage-corrected pig had values  $\geq 3$  on day 1 (0/2), but 1/2 had a ratio indicative of pancreatic leak at day 2. No values  $\geq 3$  were observed in the indicator-negative pig (0/1) throughout the experiment.

The sensitivity and specificity of SmartPAN in predicting the likelihood of pancreatic leak are shown in Table 7. Overall, the sensitivity of SmartPAN was 100% over days 1 and 2, while specificity dropped from 100% to 25% between days.

**Reassessment of indicator reaction at 48 h.** All pigs underwent a second laparotomy and re-evaluation of their peritoneal cavity at 48 h. All animals in treatment Group 1 showed signs of POPF, including cloudy

**Table 6.** Mann–Whitney pairwise comparisons of amylase content in drainage fluid at pre-operative day 0 and for two days post-pancreatic-resection. Comparison of medians is given in italics above the statistics.

Day	Group 1 vs. 2	Group 1 vs. 3	Group 2 vs. 3
0	NA	1690 vs. 553 $U_5 = 0.00, p = 0.400$	NA
1	11,345 vs. 3388 $U = 0.00, n = 9, p = 0.560$	11,345 vs. 3364 $U = 0.00, n = 8, p = 0.250$	3388 vs. 3364 $U = 1.00, n = 3, p = 1.000$
2	7019.5 vs. 5403.5 $U = 5.00, n = 8, p = 0.857$	7019.5 vs. 2356 $U = 0.00, n = 7, p = 0.286$	5403.5 vs. 2356 $U = 0.00, n = 3, p = 0.667$

**Table 7.** Sensitivity and specificity of SmartPAN for predicting the occurrence of pancreatic leaks. Leaks are diagnosed based on drainage amylase level: normal serum amylase  $\geq 3$  (Table S1).

	Day 1		Day 2	
	Leak	No leak	Leak	No leak
Indicator +ve	7	0	3	3
Indicator -ve	0	1	0	1
Sensitivity	$7/(7+0) = 1.00$		$3/(3+0) = 1.00$	
Specificity	$1/(1+0) = 1.00$		$1/(3+1) = 0.25$	

ascites, intra-abdominal abscess formation, and adhesions. These features were absent in Groups 2 and 3. Figure 7 shows perioperative photographs of the pancreatic remnants of representative pigs from each of the study groups at initial surgery (day 0) and upon laparotomy (day 2). Reapplication of SmartPAN confirmed that all animals in Group 1 continued to leak from their original sites. By contrast, we did not detect pancreatic leakage in Groups 2 and 3, nor were there any signs of pancreatitis, inflammation, and postoperative hemorrhage.

## Discussion

Pancreatic fluid is a crucial factor in the pathogenesis of postoperative pancreatic fistula (POPF), a major complication of PR. In the present study, we have detailed the development and early efficacy assessments of SmartPAN, a novel indicator of pancreatic fluid leakage designed for intraoperative use. The BTB-based hydrogel indicator takes advantage of the alkali pH of pancreatic fluid to visualize leaks following PR. Early *in vivo* experiments using a porcine model suggest that SmartPAN may reliably identify pancreatic leaks intraoperatively, facilitating targeted closure of the pancreatic remnant that stems fluid leakage for at least 48 h.

A clinically effective and usable indicator of pancreatic leakage should display the following properties: (i) a fast, durable and localized response, (ii) a clearly

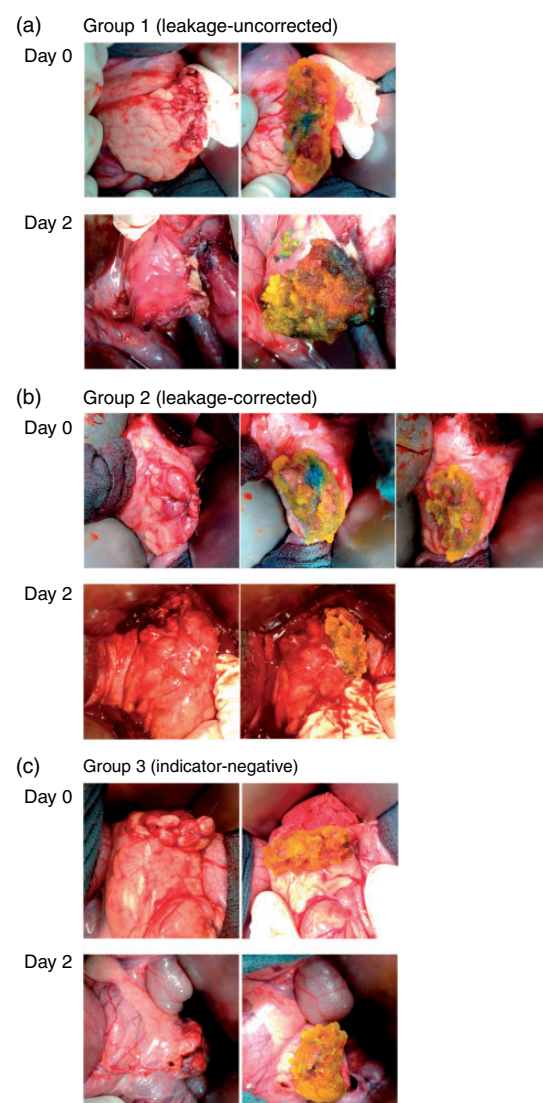


**Figure 7.** Representative images of perioperative porcine pancreatic remnants following distal pancreatectomy pre- and post-SmartPAN application on days 0 and 2. (a) Group 1 (leakage-uncorrected); (b) Group 2 (leakage-corrected); (c) Group 3 (indicator-negative). SmartPAN color change (blue) was consistent between day 0 and day 2 in all animals. Photo credits TP.

discernible color change, (iii) ease of use, (iv) high sensitivity and specificity, (v) nontoxicity. However, research and development of appropriate indicators to date have been limited. In 1998, a study group from Kyushu University, Japan applied red litmus paper to the cut surface of the human pancreas to visualize alkali pancreatic fluid.<sup>20</sup> Although too crude a method to be clinically useful, the researchers suggested that a similar technique might have an application for the identification and closure of transected pancreatic ducts. More recent studies by a group at the University of Tokyo<sup>18,19,21</sup> focused on the development of fluorescent probes that are activated by enzymes present in pancreatic fluid. Whilst their probes were able to visualize the presence of pancreatic leaks intraoperatively, the procedure requires substantial material and practical costs including installation of a specialist light source, light-blocking glasses and darkening of the operating theatre. These properties make the technique unattractive for routine usage. Finally, another team from Kyushu University<sup>17</sup> devised a Förster resonance energy transfer (FRET) heat-shock protein probe. Again, excitation of the probe and detection of the FRET signal require specialist equipment not readily available in most operating theatres. Finally, only the fluorescent probe method was shown to work directly *in vivo* at the surgical field rather than indirectly *ex vivo*.<sup>19</sup>

The gold standard SmartPAN prototypes developed here appear to provide a less complicated approach to identify and localize pancreatic leaks. The hydrogel is easy to handle and apply, and results in a rapid, localized, and durable color change upon exposure to pancreatic fluid. The color change is obvious and contrasts with intra-abdominal contents. Furthermore, our studies demonstrate that indicator reactions are consistent over a 48-hour timeframe. Close clinical observation and monitoring throughout this short study suggest that SmartPAN does not cause local or systemic toxicity, acknowledging that we flushed almost all the gel from the abdominal cavity. It should be mentioned that BTB is not considered to be toxic at the concentrations used (see the respective Material Safety Data Sheet). However, we are conducting further safety assessments to confirm the nontoxicity of SmartPAN.

We used the ratio of drainage amylase: normal serum amylase and repeated SmartPAN application at relaparotomy as prognostic indicators of pancreatic leakage. Greater levels of amylase in the abdominal drainage fluid were consistently observed in animals from leakage-uncorrected pigs, which coincide with expectations following initial surgery. While these biochemical differences did not reach statistical significance, possibly due to disproportionate group numbers and small sample size, their relevance is

supported by findings at relaparotomy. Leakage-uncorrected pigs showed early clinical signs of POPF, whereas leakage-corrected and indicator-negative pigs did not. This suggests a correlation between heightened drainage amylase and early clinical signs of POPF. It is important to reiterate at this stage that the value and reliability of the amylase data in this study are in question because guidelines suggest that amylase levels should be tracked for a minimum of three days to be diagnostic of a leakage. Additionally, concerns with group imbalance and cohort size make intergroup comparison impossible. The POPF predictive capabilities of SmartPAN will thus be the subject of future studies.

## Conclusions

The pancreatic fluid indicator described in this study may meet the need for intraoperative control of complications during PR. SmartPAN is simple to use and provides clear, localized, and rapid responses to pancreatic fluid. It may facilitate refined closure of the pancreatic remnant and adoption of appropriate postoperative management in order to reduce the risk of POPF. The findings of this study justify further investigation of SmartPAN's clinical value.

## Acknowledgments

The authors thank Harry O'Connor, Steven Walker, Samuel Waldron and Kfir Lapid at St Giles Medical GmbH and St Giles Medical Ltd. and Stephen Heap at Dr Stevil PhD for editorial support. They also thank Christian Rau at madein.io for support with figure design. Assistance was paid for by Heidelberger Stiftung Chirurgie and personal funds of first author.

## Declaration of conflicting interests

The author(s) declared the following potential conflicts of interest with respect to the research, authorship, and/or publication of this article: Expenses of two cooperative project steering-committee meetings were funded by Magle Chemoswed, Malmö, Sweden.

## Funding

The author(s) disclosed receipt of the following financial support for the research, authorship, and/or publication of this article: The technical development and *in vitro* tests were financially supported by Heidelberger Stiftung Chirurgie. *In vivo* studies were financially supported by the Medtech 4 Health Program of Vinnova Swedish Agency for Innovation.

## ORCID iD

Thomas Moritz Pausch  <https://orcid.org/0000-0001-6145-3263>

## Supplemental material

Supplemental material for this article is available online.

## References

1. Amini N, Spolverato G, Kim Y, et al. Trends in Hospital Volume and Failure to Rescue for Pancreatic Surgery. *J Gastrointest Surg.* 2015; 19: 1581–1592.
2. Kleeff J, Michalski C, Friess H, et al. Pancreatic cancer: from bench to 5-year survival. *Pancreas.* 2006; 33: 111–118.
3. Siegel RL, Miller KD and Jemal A. Cancer Statistics, 2017. *CA Cancer J Clin.* 2017; 67: 7–30.
4. Hartwig W, Hackert T, Hinz U, et al. Pancreatic cancer surgery in the new millennium: better prediction of outcome. *Ann Surg.* 2011; 254: 311–319.
5. Bassi C, Dervenis C, Butturini G, et al. Postoperative pancreatic fistula: an international study group (ISGPF) definition. *Surgery* 2005; 138: 8–13.
6. Bassi C, Marchegiani G, Dervenis C, et al. The 2016 update of the International Study Group (ISGPS) definition and grading of postoperative pancreatic fistula: 11 years after. *Surgery* 2017; 161: 584–591.
7. Bassi C, Buchler MW, Fingerhut A, et al. Predictive factors for postoperative pancreatic fistula. *Ann Surg* 2015; 261: e99.
8. Bassi C, Butturini G, Molinari E, et al. Pancreatic fistula rate after pancreatic resection. The importance of definitions. *Dig Surg* 2004; 21: 54–59.
9. Pratt WB, Maithel SK, Vanounou T, et al. Clinical and economic validation of the International Study Group of Pancreatic Fistula (ISGPF) classification scheme. *Ann Surg* 2007; 245: 443–451.
10. Xiong JJ, Tan CL, Szatmary P, et al. Meta-analysis of pancreaticogastrostomy versus pancreaticojejunostomy after pancreaticoduodenectomy. *Br J Surg* 2014; 101: 1196–1208.
11. Zhang H, Zhu F, Shen M, et al. Systematic review and meta-analysis comparing three techniques for pancreatic remnant closure following distal pancreatectomy. *Br J Surg* 2015; 102: 4–15.
12. Barreto SG, Singh A, Perwaiz A, et al. The cost of pancreaticoduodenectomy - an analysis of clinical determinants. *Pancreatology* 2016; 16: 652–657.
13. Pulvirenti A, Marchegiani G, Pea A, et al. Clinical Implications of the 2016 International Study Group on Pancreatic Surgery Definition and Grading of Postoperative Pancreatic Fistula on 775 Consecutive Pancreatic Resections. *Ann Surg* 2018; 268: 1069–1075.
14. de Reuver PR, Gundara J, Hugh TJ, et al. Intra-operative amylase in peri-pancreatic fluid independently predicts for pancreatic fistula post pancreaticoduodenectomy. *HPB (Oxford)* 2016; 18: 608–614.
15. Molinari E, Bassi C, Salvia R, et al. Amylase value in drains after pancreatic resection as predictive factor of postoperative pancreatic fistula: results of a prospective study in 137 patients. *Ann Surg* 2007; 246: 281–287.
16. Ecker BL, McMillan MT, Allegrini V, et al. Risk factors and mitigation strategies for pancreatic fistula after distal pancreatectomy: analysis of 2026 resections from the International, Multi-institutional Distal Pancreatectomy Study Group. *Ann Surg* 2019; 269: 143–149.
17. Hamano N, Murata M, Kawano T, et al. Förster resonance energy transfer-based self-assembled nanoprobe for rapid and sensitive detection of postoperative pancreatic fistula. *ACS Appl Mater Interfaces* 2016; 8: 5114–5123.
18. Kuriki Y, Kamiya M, Kubo H, et al. Establishment of molecular design strategy to obtain activatable fluorescent probes for carboxypeptidases. *J Am Chem Soc* 2018; 140: 1767–1773.
19. Mori K, Ishizawa T, Yamashita S, et al. Intraoperative visualization of pancreatic juice leaking from the pancreatic stump in a swine model. *Gastroenterology* 2015; 149: 1334–1336.
20. Yamaguchi K, Chijiwa K, Shimizu S, et al. Litmus paper helps detect potential pancreateoenterostomy leakage. *Am J Surg* 1998; 175: 227–228.
21. Yamashita S, Sakabe M, Ishizawa T, et al. Visualization of the leakage of pancreatic juice using a chymotrypsin-activated fluorescent probe. *Br J Surg* 2013; 100: 1220–1228.
22. Dimick JB, Sedrakyan A and McCulloch P. The IDEAL framework for evaluating surgical innovation: how it can be used to improve the quality of evidence. *JAMA Surg* 2019. DOI: 10.1001/jamasurg.2019.0903.
23. McCulloch P, Altman DG, Campbell WB, et al. No surgical innovation without evaluation: the IDEAL recommendations. *Lancet* 2009; 374: 1105–1112.
24. McCulloch P, Cook JA, Altman DG, et al. IDEAL framework for surgical innovation 1: the idea and development stages. *BMJ* 2013; 346: f3012.
25. Hamm LL, Nakhol N and Hering-Smith KS. Acid-base homeostasis. *Clin J Am Soc Nephrol* 2015; 10: 2232–2242.
26. Ohya I, Iwasa M, Komoriya H, et al. Identification of human saliva by antisera to alpha-amylase in human salivary glands. *Tohoku J Exp Med* 1986; 150: 309–315.
27. European Commission. Clinical evaluation: a guide for manufacturers and notified bodies under directives 93/42 and 90/385. 2016.
28. American Heart Association. Part 1: Introduction to the International Guidelines 2000 for CPR and ECC: a consensus on science. *Circulation* 2000; 102: 1–11.
29. Takada T, Yasuda H, Hasegawa H, et al. Use of brom-thymol blue, a pH indicator, for detecting the pancreatic duct orifice after resection of the head of the pancreas. *J Hep Bil Pancr Surg* 1995; 2: 401–405.